Coral Reefs (2012) 31:521–534
DOI 10.1007/s00338-011-0868-6

REPORT

Diel rhythmicity of lipid-body formation in a coral-*Symbiodinium* endosymbiosis

W.-N. U. Chen · H.-J. Kang · V. M. Weis · A. B. Mayfield · P.-L. Jiang · L.-S. Fang · C.-S. Chen

Received: 7 August 2011 / Accepted: 16 December 2011 / Published online: 30 December 2011

Abstract The biogenesis of intracellular lipid bodies (LBs) is dependent upon the symbiotic status between host corals and their intracellular dinoflagellates (genus *Symbiodinium*), though aside from this observation, little is known about LB behavior and function in this globally important endosymbiosis. The present research aimed to understand how LB formation and density are regulated in the gastrodermal tissue layer of the reef-building coral *Euphyllia glabrescens*. After tissue fixation and labeling with osmium tetroxide, LB distribution and density were quantified by imaging analysis of serial cryo-sections, and a diel rhythmicity was observed; the onset of solar irradiation at sunrise initiated an increase in LB density and size, which peaked at sunset. Both LB density and size then decreased to basal levels at night. On a seasonal timescale, LB density was found to be significantly positively correlated with seasonal irradiation, with highest densities found in the summer and lowest in the fall. In terms of LB lipid composition, only the concentration of wax esters, and not triglycerides or sterols, exhibited diel variability. This suggests that the metabolism and accumulation of lipids in LBs is at least partially light dependent. Ultrastructural examinations revealed that the LB wax ester concentration correlated with the number of electron-transparent inclusion bodies. Finally, there was a directional redistribution of the LB population across the gastroderm over the diel cycle. Collectively, these data reveal that coral gastrodermal LBs vary in composition and intracellular location over diel cycles, features which may shed light on their function within this coral–dinoflagellate mutualism.

Keywords Cnidaria · Diel rhythm · Gastroderm · Lipid droplets · Osmium tetroxide · Symbiosis

Communicated by Biology Editor Dr. Mark Warner

W.-N. U. Chen
Department of Biological Science and Technology, I-Shou University, Kaohsiung, Taiwan, ROC

H.-J. Kang · A. B. Mayfield · P.-L. Jiang · C.-S. Chen
Graduate Institute of Marine Biotechnology, National Dong-Hwa University, Checheng, Pingtung 944, Taiwan, ROC

H.-J. Kang · A. B. Mayfield · P.-L. Jiang · C.-S. Chen (✉)
Taiwan Coral Research Center (TCRC), National Museum of Marine Biology and Aquarium, Checheng, Pingtung 944, Taiwan, ROC
e-mail: cchen@nmmba.gov.tw

V. M. Weis
Department of Zoology, Oregon State University, Corvallis, OR, USA

L.-S. Fang
Department of Sport, Health and Leisure, Cheng-Shiu University, Kaohsiung, Taiwan, ROC

C.-S. Chen
Department of Marine Biotechnology and Resources, National Sun Yat-Sen University, Kaohsiung, Taiwan, ROC

Introduction

Mutualistic associations between dinoflagellates (*Symbiodinium* sp.) and cnidarians (e.g., corals and sea anemones) are ecologically important and are responsible for the construction of coral reefs. As such, they have been the subject of intensive investigation during the past decades at the ecological scale (LaJeunesse et al. 2010). However, microscale investigations of the symbiosis at the cell and molecular levels have been slower to arrive, due in part to the challenges inherent in studying intimate endosymbioses

(Weis et al. 2008; Weis and Allemand 2009). Given the looming threats of global climate change on coral reef ecosystems, there is an urgent need to better understand the basic biology of these fundamentally important endosymbioses.

The coral–*Symbiodinium* association is an endosymbiosis in which the dinoflagellate symbionts reside within the anthozoan host's gastrodermal cells and contribute to the latter's nutrition by translocating photosynthetically fixed carbon and other metabolites into the host cytoplasm (Whitehead and Douglas 2003). Thus, one of the critical steps in understanding this endosymbiosis is to examine the nature of the energy flow between *Symbiodinium* and their hosts. Whereas many studies have described the production and translocation of glycerol and amino acids within the coral holobiont, only a few have examined the role of lipid synthesis and transport. Electron microscopic examinations of *Symbiodinium* in the coral *Acropora acuminata* suggested that the endosymbionts represent the primary site of lipid synthesis, and these lipids are translocated to the host tissues (Crossland et al. 1980). Other analyses examining the apparent translocation of radio-labeled (^{14}C) lipids between *Symbiodinium* and coral hosts during the circadian photoperiod have been inconclusive (Kellogg and Patton 1983; Patton and Burris 1983). Several studies have described the presence of lipid bodies (LBs, also referred to as "lipid droplets") in host cells that house *Symbiodinium*. It has been hypothesized that these bodies are lipid reservoirs generated during the endosymbiotic process (Kellogg and Patton 1983; Patton and Burris 1983; Patton et al. 1983), though their exact function remains unclear (Muscatine et al. 1994).

In a variety of bacterial, plant, and invertebrate and vertebrate cells, LBs are specific lipid-storage organelles (Olofsson et al. 2009) that originate in the endoplasmic reticulum (ER) (Robenek et al. 2006; Wan et al. 2007; Ohsaki et al. 2009). Neutral lipids are synthesized between the leaflets of the ER membranes and, eventually, mature LBs bud from the ER to form atypical organelles containing a monolayer of phospholipids with a unique fatty acid composition (Tauchi-Sato et al. 2002). Recent proteomic analyses have demonstrated that LBs not only function as a lipid reservoirs, but are also involved in a vast array of other cellular processes (Welte 2007), including lipid metabolism (Duncan et al. 2007), cholesterol homeostasis (Prattes et al. 2000; Maxfield and Tabas 2005), membrane trafficking (Liu et al. 2004; Ozeki et al. 2005), cell signaling (Umlauf et al. 2004), regulation of transcription and translation (Fujimoto et al. 2004), and embryonic development (Cermelli et al. 2006).

In comparison to lipid droplets of other eukaryotic cells, recent studies have found that coral gastrodermal LBs are unique in both morphology and molecular composition, and their presence is dependent upon endosymbiotic status (Luo et al. 2009; Peng et al. 2011). For instance, in healthy specimens of the stony coral *Euphyllia glabrescens*, most lipids generated by *Symbiodinium* were transferred to the host coral LBs (Luo et al. 2009). However, upon high temperature-induced bleaching, lipid export to the host cell LB was retarded, resulting in a concurrent decrease in LB density and a change in their composition (Luo et al. 2009). Ultrastructural analyses of host coral LBs in situ showed that they exhibit defined morphological characteristics, including a high electron density resulting from a distinct lipid composition in comparison to the lipid droplets of mammalian cells (Peng et al. 2011). They were also characterized by the presence of numerous electron-transparent inclusion bodies of unknown origin and composition. Both proteomic and ultrastructural observations seem to suggest that both *Symbiodinium* and host organelles, such as the ER, are involved in LB biogenesis (Peng et al. 2011).

Given these findings, the relationship between LB formation and regulation of the endosymbiosis appears to be intimate, and, as such, the present study aimed to examine the in situ distribution, morphology, and composition of gastrodermal LBs across both diel cycles and seasons in *E. glabrescens*.

Materials and methods

Reagents

All filtered seawater (FSW) used for the study was prepared by filtering seawater through a VacuCap 90 filter unit (0.2 μm, Pall Gelman Laboratory, Ann Arbor, MI, USA). Artificial seawater (ASW) was prepared with 420 mM NaCl, 26 mM $MgSO_4$, 23 mM $MgCl_2$, 9 mM KCl, 9 mM $CaCl_2$, 2 mM $NaHCO_3$, and 10 mM HEPES (pH 8.2). The osmolarity of all solutions used for the treatment of cells was measured using a Micro-Osmometer (Advanced Instruments, Inc., Norwood, MA, USA) and adjusted to 1,000 mOsmol by addition of NaCl. All chemicals for cell fixation and lipid extractions were of analytical grade, and their commercial sources are noted in the text.

Coral collection and maintenance

Colonies of *Euphyllia glabrescens* (Fig. 1b, 7.2–35.8 cm in diameter) were collected by SCUBA divers from the inlet of the third nuclear power plant (21°57.376′N, 120°45.291′E) at a depth of 3–8 m in Nanwan Bay, Taiwan. They were placed in an upright position in a 4-ton outdoor tank with flow-through seawater (exchange rate of

~80 l/h) and were maintained under a natural photoperiod with additional air circulation in the husbandry center of the National Museum of Marine Biology and Aquarium (NMMBA). A microprocessor-controlled cooler (First FC-45, Aquatech, Kaohsiung, Taiwan) was linked to the tank, and the temperature was maintained at 26.5 ± 1°C (standard deviation of the mean). The light intensity and water temperature were continuously recorded using a data logger (HOBO Temperature/Light Pendant Data Logger, UA-002; Onset Computer Corporation, Pocasset, MA, USA) that was placed near the colonies.

Sampling of coral tentacles and labeling of gastrodermal lipid bodies with osmium tetroxide

Tentacles were amputated from the polyps of the *E. glabrescens* colonies using curved surgical scissors (9 cm, Mede Technik, Emmingen, Germany). In an individual experiment, 5–10 tentacles with a stretched length of ~3 cm were collected at each time point during the 24-h diel cycle from three coral colonies, and no colony was amputated more than once in any experiment to avoid stress and aberrant behavior caused by the amputation process. Two or three tentacles were used for detection of LBs by osmium tetroxide labeling (see below). The others were processed for gastrodermal LB isolation and lipid analysis.

After amputation, tentacles were immediately rinsed with FSW and anesthetized sequentially with 3.5 and 7% $MgCl_2$ (in FSW, 10 min each). They were then fixed with 3.6% paraformaldehyde (in PBS; Sigma-Aldrich, MO, USA) for 3 h at 4°C, followed by triplicate PBS rinses to remove fixative. The gastrodermal LBs in fixed tentacles were labeled by 1% osmium tetroxide (in PBS; Electron

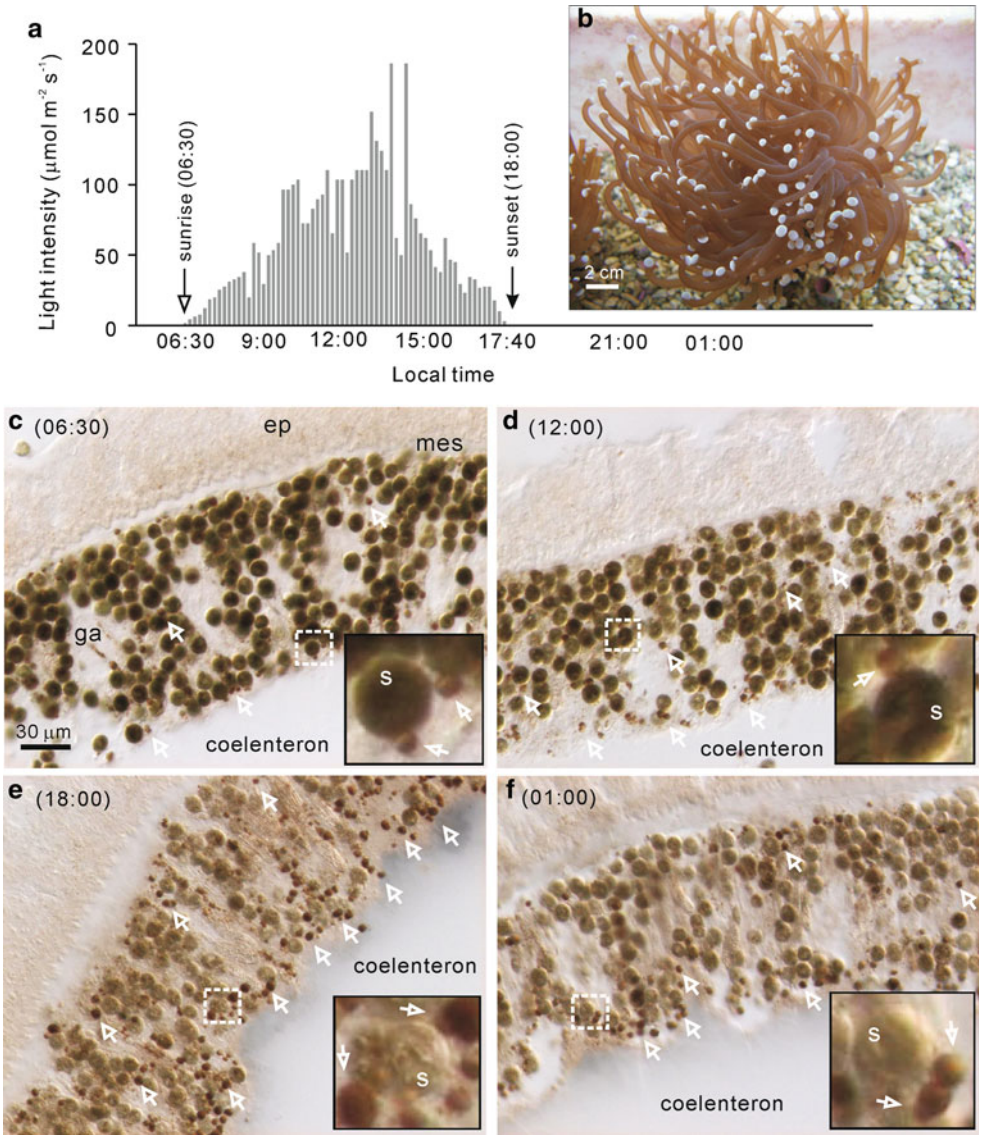

Fig. 1 Osmium tetroxide labeling of gastrodermal lipid bodies (LBs) in tentacles of *Euphyllia glabrescens* over a diel cycle. **a** A representative diel light intensity change in the coral culture tank during spring. *Blank* and *filled arrows* indicate times of sunrise and sunset, respectively. **b** A colony of the stony coral *E. glabrescens* with extended tentacles. **c–f** Microscopic images of tentacle cryo-sections labeled with osmium tetroxide at different times (**c** 06:30 hours; **d** 12:00 hours; **e** 18:00 hours; **f** 01:00 hours). Both *Symbiodinium* (*s*) and LBs (indicated by *blank arrows*) are visible in the gastroderm (*ga*), but not the epiderm (*ep*) or mesoglea (*meso*). Selected regions (see the *dashed line squares*) are magnified and shown in *insets* to demonstrate the diel change in osmium tetroxide labeling intensity in the endosymbionts

Microscopy Sciences, Hatfield, PA, USA) at room temperature (RT) for 2 h. Excess osmium tetroxide solution was then removed by triplicate washes of fresh PBS (10 min each).

Cryo-sectioning and gastrodermal LB density analysis

Cryo-protection was conferred by infiltrating the fixed and labeled tentacles with OCT compound (tissue freezing medium, R. Jung GmbH, Nussloch, Germany) for 1 h at RT, followed by embedding in the same medium at −30°C for 1 h prior to sectioning. Since there are almost no *Symbiodinium* or LBs in the tip region of the tentacles, the orientation of the processed tentacles was adjusted to allow serial cross-sections (10 μm thickness) starting from the amputated region using a Leica CM 1850 Cryostat (Leica Microsystems, Nussloch GmbH, Heidelberg, Germany). The sections were placed onto polylysine pre-coated slides (Polyscience, Menzel, Germany), washed with ddH_2O three times to remove OCT, and then mounted with ddH_2O for immediate observation and image acquisition using microscopy. In some cases, sections were mounted with the antifade reagent ProLong® Gold (Invitrogen, Carlsbad, CA, USA).

Differential interference contrast (DIC) microscopy was performed using an upright microscope (Axioskop 2 plus, Zeiss) equipped with a Plan-Neofluar® (1.3 N.A.) objective. Image-Pro Plus® software (version 6.0; Media Cybernetics, Inc., Bethesda, MD, USA) was used to control the image acquisition with a CCD camera (Quantix or CoolSNAP-Pro*cf*, Photometrics Ltd., Tucson, AR, USA) using suitable exposures. Among more than 60 sections from each amputated tentacle collected at different time points, 30 DIC images containing the epiderm, mesoglea, and gastroderm were arbitrarily selected for the analysis of LB density. Since LB formation is endosymbiosis dependent (Luo et al. 2009), the gastrodermal LB density of each image was normalized to the endosymbiont density of that image.

Analysis of nocturnal LB utilization

The LB utilization during the night was examined based on the diel changes in LB density described above. Briefly, percent decrease in LB density in tentacles sampled at sunrise compared to those sampled at the previous sunset was calculated. The rate of the LB utilization was expressed as percent LB decrease per nocturnal hour. Given that only small percentage of LBs was found to be released (1–1.7%, personal observation) from the gastroderm, the assumption was made that the nocturnal LB decrease was suggestive of utilization (e.g., metabolism) by the coral.

Analysis of LB distribution in the gastroderm

To measure the gastrodermal distribution of LBs, DIC images of tentacle cryo-sections were first acquired as described above. The gastroderm was divided into three regions of equal width, including "meso" (the region most proximal to the mesoglea), "mid" (the interior region of the gastroderm), and "coe" (the region adjacent to the coelenteron). The percentage of LBs in each of these regions was quantified (see also the legend of Fig. 6).

LB isolation and lipid analysis

Five to seven amputated tentacles of *E. glabrescens* were collected as described above. After rinsing with FSW, tentacle tips were removed using microscissors (Spring Type, AESCULAP Inc., Center Valley, PA, USA) to prevent interference from nematocytes. The gastroderm was then separated from the epiderm by incubation with 3% *N*-acetylcysteine (pH 8.2, prepared in ASW) for 1–2 h at RT (Peng et al. 2008), and isolated gastroderms were homogenized on ice using a 7-ml glass tissue grinder (Kimble/Kontes, Vineland, NJ, USA) at 20–30 passes in 1 ml homogenization buffer (250 mM sucrose in ASW, pH 8.2). Under such homogenization, gastrodermal cells were broken to release their intracellular LBs, while *Symbiodinium* cells remained intact.

The homogenate was then centrifuged (500×*g* at 4°C for 10 min), and the LB-containing supernatant was collected. To release LBs trapped in the pellet, the precipitate was vortexed with 0.5 ml ASW containing 250 mM sucrose and centrifuged as above. The washing process was repeated until no LBs appeared in the supernatant. Protein concentration in the pooled supernatant fraction (representing host tissues) was measured with the BCA protein assay kit (Pierce, IL, USA). All supernatant fractions were pooled and centrifuged at 15,000×*g* at 4°C for 90 min, and the topmost layer containing LBs was collected.

The purity of the LB fractions was examined by Western blot using primary antibodies specific for contaminating proteins from both host cells (ADP ribosylation factor [ARF] and actin) and *Symbiodinium* (Rubisco). Briefly, LBs were delipidated according to the procedure described by Mastro and Hall (1999), and the remaining proteins were quantified with a 2-D Quant Kit (80-6483-56, GE Healthcare, Waukesha, WI, USA). Ten micrograms (10 μg) of protein were subjected to 12% SDS-PAGE using a Bio-Rad Mini-PROTEAN 3 system (Bio-Rad, Hercules, CA, USA). After separation by SDS-PAGE, Western blots were performed as previously described (Peng et al. 2010) using the following monoclonal, primary antibodies: rabbit anti-Rubisco large subunit (1:2,000 dilution; Agrisera, Vannas, Sweden), mouse anti-actin (1:4,000 dilution,

Millipore, Billerica, MA, USA), and mouse anti-ARF (1:500 dilution, Abcam, Cambridge, MA, USA).

Lipid contents of LB fractions were extracted as in Bligh and Dyer (1959) and subjected to either silica HPTLC (10×10 cm^2, silica gel 60 F_{254}, E. Merck, Whitehouse Station, NJ, USA) or TLC (20×20 cm^2, F_{254}, Analtech, Newark, DE, USA), with six repetitions for each extract. Chromatography was sequentially developed by two solvent systems modified from previous reports (Oku et al. 2003; Fuchs et al. 2007). Briefly, TLC was first developed to the retention factor (R_f) = 0.5 position by chloroform:ethanol:H_2O:triethylamine (35:35:7:35, v/v/v/v). The plate was air-dried and then developed to the top ($R_f = 1$) using hexane: diethyl ether: acetic acid (70:30:1, v/v/v). Lipid standards for wax esters (WE), sterols (ST), triglycerides (TG), fatty acids (FA), and phospholipids were palmityl palmitate, cholesterol, tripalmitin, palmitic acid, phosphatidylethanolamine, phosphatidylcholine and lysophosphatidylcholine, respectively (from Sigma-Aldrich or Matreya Inc., Pleasant Gap, PA, USA).

Lipid visualization on TLC plates was achieved by staining with 0.03% Coomassie blue R 250 (in 20% methanol containing 0.5% acetic acid) (Abe 1998). Staining intensities and R_f of lipid spots were then determined using the Metamorph® Image Processing system (Molecular Devices, Inc., Toronto, Canada). Lipid species concentrations were normalized to total, coextracted host gastrodermal protein.

Transmission electron microscopy and imaging analyses

To investigate the LB structure, tentacles were fixed in 2.5% glutaraldehyde/2% paraformaldehyde/100 mM sodium phosphate containing 5% sucrose (pH 7.3) for 2.5 h at 4°C, then washed with 100 mM sodium phosphate at 4°C. They were then post-fixed in 1% osmium tetroxide in 50 mM sodium phosphate (pH 7.3) for 1 h at 4°C. The tissue blocks were washed with water, dehydrated with increasing concentrations of ethanol (50, 70, 80, 90, 95, and 100%), and embedded in Spurr's resin (Electron Microscopy Sciences). Sections were then post-stained in 2.5% uranyl acetate in methanol with 0.4% lead citrate and deposited onto copper grids before air-drying. Samples were imaged using a JEM-1400 TEM (JEOL, Japan). Micrographs were taken by a CCD camera (Orius™ SC1000W, model 832, Gatan, Inc., Pleasanton, CA, USA), and image analyses were performed with Metamorph 6.3 software (Molecular Devices).

In order to determine LB area (or size) from the acquired images, the ratio of actual length to pixel was first determined by distance calibration using the scale bar of the acquired TEM image. Individual LBs were selected by threshold adjustment, and the area (μm^2) of individual LBs was calculated with Metamorph's region measurement function. To calculate the percentage area of electron-transparent inclusion bodies (ETIs) in individual LBs, threshold levels of the image were adjusted to create a masking of the total inclusions. The areas of the ETIs were then calculated as with the LBs.

Statistics

Data were analyzed with the Statistical Package for the Social Sciences (version 14.0, IBM, Armonk, NY, USA). One-way analysis of variance (1-way ANOVA) and Duncan's multiple range tests were utilized, and results were deemed statistically significant, if $P < 0.05$. Values are presented as mean ± standard error of the mean (SEM).

Results

The spatio-temporal dynamics of coral LBs were assessed by tracking LB size, density, and distribution during the diel photoperiod and in different seasons with osmium tetroxide labeling of fixed tissues. Osmium tetroxide preferentially reacts with the unsaturated bonds of lipids and imparts an electron density that is both correlated with the number of unsaturated bonds and observable with light and electron microscopy (D'Avila et al. 2006; Cheng et al. 2009).

Diel changes in gastrodermal LB density in coral tentacles

The distribution of LBs in tentacles was examined during a representative diel cycle in the spring (Fig. 1). Osmium tetroxide clearly labeled both *Symbiodinium* and LBs (arrows of Fig. 1c–f) in the gastroderm. At sunrise (06:30 hours; Fig. 1c), both endosymbionts and LBs were heavily labeled by osmium tetroxide, and LBs appeared to be concentrated around the endosymbionts (magnified inset of Fig. 1c). Osmium tetroxide labeling of both LBs and *Symbiodinium* in the gastrodermal cells was further confirmed by transmission electron microscopy (TEM, Fig. 5). On the other hand, staining was minimal in the epidermis, which contained neither LBs nor *Symbiodinium*.

At the second sampling time, (12:00 hours, Fig. 1d), which was characterized by a higher light intensity (Fig. 1a), more LBs appeared around the endosymbionts (blank arrows of Fig. 1d), and osmium tetroxide staining of *Symbiodinium* decreased (inset of Fig. 1d) relative to 06:30 hours values. In contrast, at sunset (18:00 hours, Fig. 1e), numerous LBs labeled by osmium tetroxide

appeared (blank arrows of Fig. 1e). Specifically, LB density along the gastrodermal border adjacent to the coelenteron increased drastically. Furthermore, though the osmium tetroxide labeling intensity of LBs remained dense, the staining of *Symbiodinium* significantly decreased. At night (01:00 hours), the number of LBs decreased (Fig. 1f), although a significant number of LBs still remained in regions adjacent to the coelenteron. The staining of *Symbiodinium* was also less than in tentacles sampled at 06:30 hours.

To quantify potential diel variability in gastrodermal LB density, tentacles were sampled every 3 h for 2 days in four different seasons. Since the formation of gastrodermal LBs is endosymbiosis dependent (Luo et al. 2009), the LB density was normalized to the *Symbiodinium* density of the respective micrograph. LB density was found to correlate significantly with light intensity (Fig. 2); in all seasons, LB density started to increase at sunrise (blank arrows of Fig. 2) and gradually rose over the course of the day, reaching maximum density at sunset (filled arrows, Fig. 2). When the time of sunset occurred later in the day, such as in spring (18:30 hours) and summer (19:00 hours), the time at which LB density reached a maximum level was correspondingly delayed (dashed line of Fig. 2). The LB densities then decreased to initial levels over the duration of the night.

The integrated diel light intensity measured over 2 days in different seasons was highly correlated with the daily maximum LB density, which always occurred at sunset (Fig. 3a). Tentacles sampled in the summer contained the highest LB density (1.32 ± 0.07), while LB densities in the spring (1.07 ± 0.03), winter (0.96 ± 0.04), and fall (0.90 ± 0.04) were significantly lower.

Given the diel fluctuations in LB density (Fig. 2), it was hypothesized that the decrease in LBs over the course of the evening was indicative of LB utilization by the coral. To further emphasize this, the nocturnal utilization (i.e., metabolism) of LBs, which could not be observed over the daylight hours as LBs were concurrently forming during such times, was measured (Fig. 3b). There was significant LB utilization at night, with decreases in LB density ranging from ~48 to ~63%. The LB utilization percentages were not correlated with the integrated light intensity and showed no significant difference among seasons. However, further analyses (Fig. 3c) indicated that the rate of LB utilization in summer ($6.25 \pm 1.47\%$ per hour) was significantly faster (1-way ANOVA, effect of season $P < 0.001$) than those in other seasons.

Diel changes in LB lipid composition and ultrastructural morphology

LBs were purified specifically from the gastroderm after tissue separation by 3% NAC treatment at 3-hour intervals over a 2-day period (Fig. 4). The homogenization process lysed the gastrodermal cells and released LBs, though did not damage the *Symbiodinium* cells (Peng et al. 2011). Afterward, low buoyant density LBs (average size, 3.47 ± 0.04 μm) were isolated by centrifugation (Fig. 4a). Their purity was then confirmed by both high lipid content (as assessed by thin layer chromatography [TLC]) and absence of contaminating host and *Symbiodinium* proteins (as assessed by Western blot; Peng et al. 2011). Coomassie blue staining-based lipid analyses (Fig. 4b) showed that LBs were highly concentrated with wax esters (WE), triglycerides (TG), sterols (ST), and phospholipids (PE, PC, and lysoPC). Western blot analyses confirmed that the isolated LB fraction was devoid of marker proteins of the host (ARF and one of the two actins) and *Symbiodinium* (Rubisco) (Fig. 4c). However, purified LBs were shown to contain an intrinsic, ~45-kDa actin.

Diel changes in WE, TG, and ST concentrations in LBs were investigated. In general, the concentrations of the individual lipid species (Fig. 4d) correlated with LB density (Fig. 2). Lipid concentrations (μg per 100 μg host protein) started to increase at sunrise (blank arrows of Fig. 4d), reached maximum levels at sunset (filled arrows of Fig. 4d), and decreased to the baseline level during the evening. As such variation could simply be a reflection of the LB density changes, their weight percentages (relative to the total mass of the three dominant lipid species; wt%) were also compared (insets of Fig. 4d). These data revealed that, in fact, only WE levels changed significantly over time (1-way ANOVA effect of time, $P < 0.001$), showing a diurnal increase followed by a nocturnal decrease. On the other hand, the weight percentage of neither TG ($P = 0.854$) nor ST ($P = 0.721$) exhibited significant diel variation.

TEM was used to more finely denote LB morphology (Fig. 5). At sunrise (06:30 hours; Fig. 5a), LBs were single globules (filled arrows) with few or no rectangular, electron-transparent inclusion bodies (ETIs, blank arrowhead). However, drastic morphological changes in LBs were observed in tentacles collected at sunset (18:00 hours; Fig. 5b), in which LBs became larger, more irregularly shaped, and tended to fuse with other LBs through a connective bridge (blank arrows, Fig. 5b). Furthermore, the number of ETIs greatly increased. These observations were further confirmed by software-based imaging analyses (Table 1), which revealed that both LB size and percentage of LB area occupied by ETIs varied significantly over diel cycles. Specifically, LB size gradually increased from 3.10 μm^2 at sunrise (06:30 hours), to a maximum of 10.61 μm^2 at sunset, and then to the initial level (4.02 μm^2) at night (01:00 hours). These sizes appear to correlate with the area percentage of ETIs (Table 1).

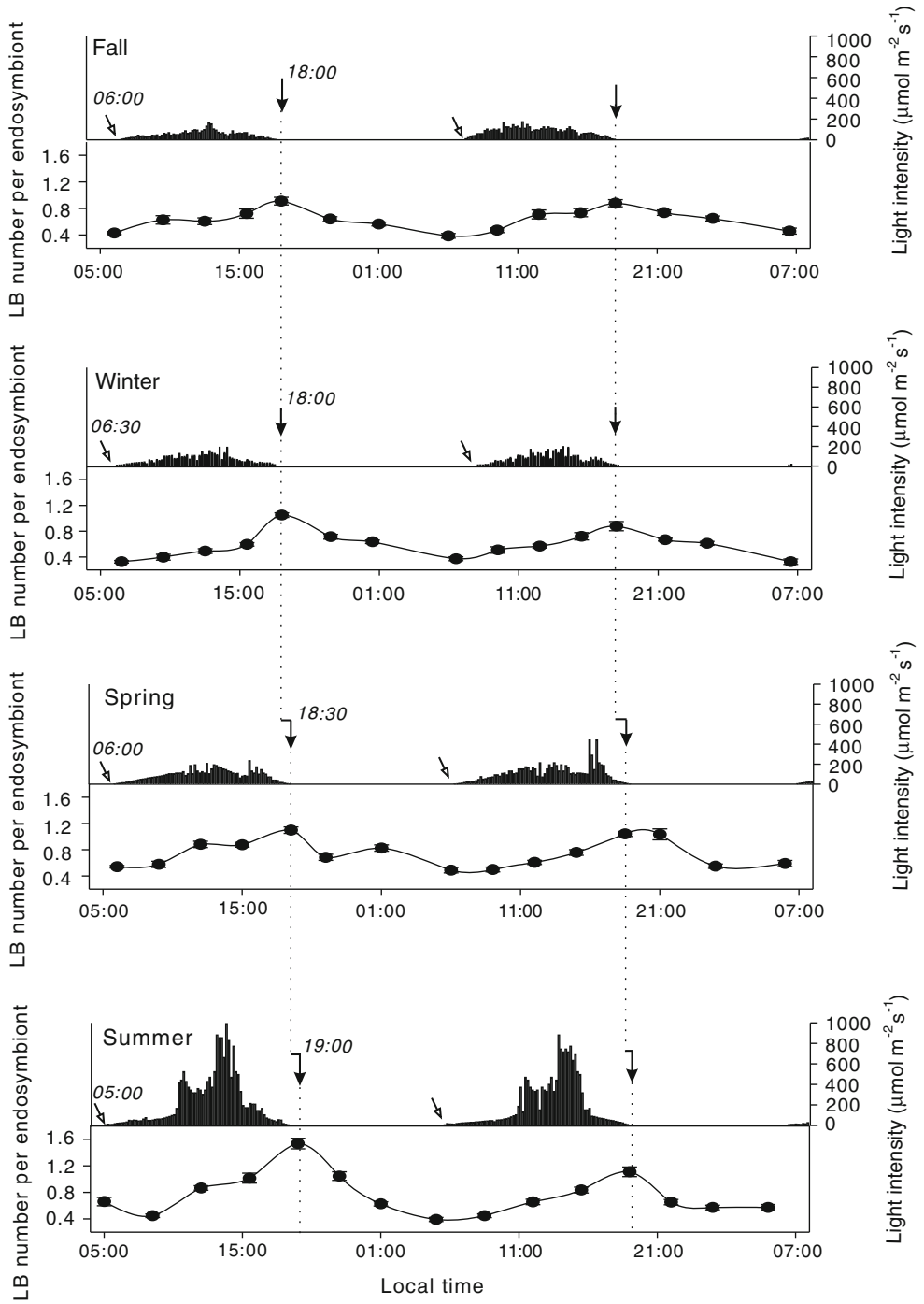

Fig. 2 Diel changes in LB density in different seasons. Representative LB density (expressed as "LB number per endosymbiont") changes in tentacles of *E. glabrescens* in the fall, winter, spring, and summer. Ten cryo-sectioned micrographs were analyzed form each of 5–10 tentacles from three coral colonies sampled at each time, and no colony was amputated more than once in any experiment. Similar results for each season were acquired from six different experiments. The LB density started to increase at the time of sunrise (indicated by *blank arrows*) and reached the maximum at sunset (indicated by *filled arrows*). They then decreased to the initial level during the night

LB redistribution

LBs in tentacles collected at sunset (Fig. 1e) were highly concentrated along the gastrodermal border with the coelenteron and thus appear to have migrated from their more central location in the tissue layer observed at the daytime sampling times (Fig. 1c–d). This putative redistribution of LB populations across the gastroderm was further analyzed (Fig. 6). First, the gastroderm was divided into three regions of equal width (red lines of Fig. 6a), including the

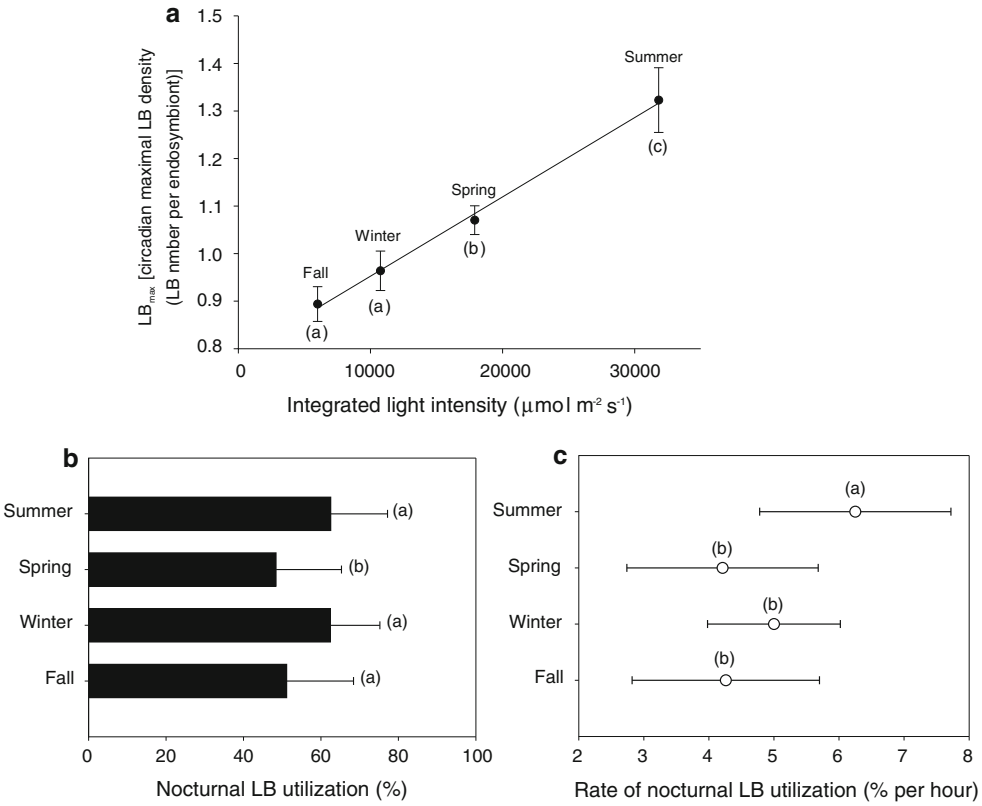

Fig. 3 Daily maximum LB density and nocturnal LB utilization in different seasons. **a** The integrated diel light intensity across seasons is highly correlated with the maximal LB density at sunset. **b** Nocturnal LB utilizations in four seasons was calculated based on Fig. 2 and expressed as the percent decrease in LB density at sunrise in comparison to that at sunset of the previous day. **c** Rates of LB utilization were examined by comparing the percent decrease per nocturnal hour (summer: 10 h; spring: 11.5 h; winter: 12.5 h; fall: 12 h). Data are presented as mean ± SEM ($n = 20$). *Parentheses a–c* denotes statistical significance between different seasons as analyzed by ANOVA

"meso" (the region closest to the mesoglea), "mid" (the middle region), and "coe" (the region adjacent to the coelenteron). The percentage of LBs in each of these three regions at 3–4-h intervals over a 2-day circadian photoperiod was then calculated (Fig. 6b). The results were averaged from four experiments, which were conducted in the spring (April 10-12), summer (June 30–July 1), fall (October 8–10), and winter (February 6–8) of 2010. A representative light intensity spectrum from the summer experiment was selected to demonstrate the general change in photoperiod for all experiments (dashed line and right *y*-axis of Fig. 6b).

There was a dynamic diel change in LB distribution within the gastroderm. The majority of LBs (more than ~50%) were found in the "coe" region throughout the diel cycle. Nevertheless, the LB percentage in this region gradually increased after sunset (filled arrows of Fig. 6b) and reached a maximum at 01:00 hour. During the night (phases I and III), 60-80% of the LBs remained in the "coe" region, decreasing to ~65% at sunrise (blank arrow) and 50%, the minimum level, at 15:30. The percentage of LBs in the "meso" and "mid" regions was around 20–55%. During the daytime (phase II), the percentage of LBs in each of these regions increased with increasing light intensity, with LBs relatively evenly distributed between them. However, the percentage of LBs in both of these regions started to decrease at sunset and reached a minimum level before sunrise (blank arrows of Fig. 6b). Furthermore, the percentage of LBs in the "meso" region was significantly smaller ($P < 0.05$) than that of the "mid" region during 22:00–01:00 hours window. Collectively, these data indicate a redistribution of LBs from the "meso" to the "mid" and to the "coe" region.

Discussion

The lipid-reactive compound osmium tetroxide was chosen as a marker for intracellular LB observation in coral tentacle tissues, given its previously determined ability to clearly resolve macrophage LBs (0.5–1 μm diameter) under light microscopy (D'Avila et al. 2006). Osmium tetroxide specifically stained LBs and *Symbiodinium* with a dark brown color under DIC (Fig. 1). No significant osmium tetroxide labeling was observed in the epidermis, where LBs and *Symbiodinium* are absent. Moreover, there was no light-induced change in osmium tetroxide staining during the experimental processes. These results demonstrate that osmium tetroxide can be used to identify LB distribution accurately under both DIC and TEM (Fig. 5). Fluorescent probes, such as nile red, oil red, and BODIPY (4,4-difluoro-4-bora-3a,4a-diaza-s-indacene) 493/503, have been used to label lipid droplets in cultured cells and tissue sections (Fowler and Greenspan 1985; DiDonato and

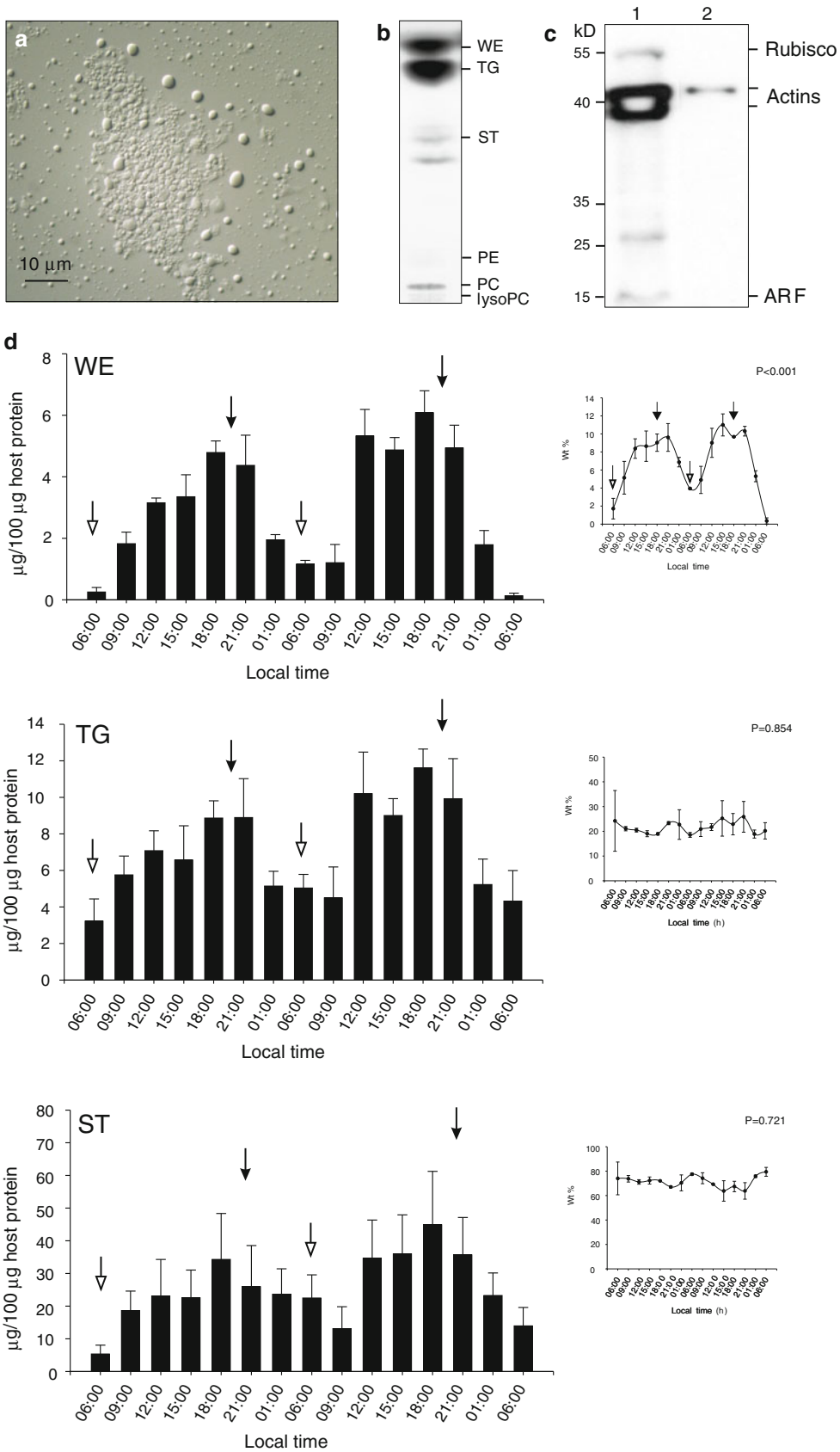

Fig. 4 Lipid analyses of LBs over the diel photoperiod. **a** Isolated LBs under DIC microscopy. **b** The purity of the LB fractions was confirmed by their high density of major neutral lipids (*WE,* wax esters; *TG,* triglycerides; *ST,* sterols) and other polar phospholipids (phosphatidylethanolamine, PE; phosphatidylcholine, PC; lysophosphatidylcholine, lysoPC). **c** Western blots were used to further demonstrate the purity of the isolated LBs. The host gastrodermal homogenate (*lane 1*) contained a protein from *Symbiodinium* (Rubisco, MW ~ 55 kDa) and two from the host (an actin doublet, MW ~ 42 and 39kDa; ARF, MW ~ 15 kDa). While three of these contaminating proteins were absent in the isolated LB fraction (*lane 2*), a host actin (MW ~ 42 kDa) was still detected, indicating that it may be an intrinsic protein of the LB (Peng et al. 2011). **d** Diel changes in concentration of three lipid species; WE, TG, and ST, in LBs isolated from host gastrodermal tissues (per 100 µg host protein) sampled over a 48-h period. *Blank* and *filled arrows* indicate the time of sunrise and sunset, respectively. The *inset* on the *right* of each lipid species indicates the diel change of the respective lipid species as a weight percentage of the total mass of the three dominant LB lipid species. Data are presented as mean ± SEM ($n = 6$)

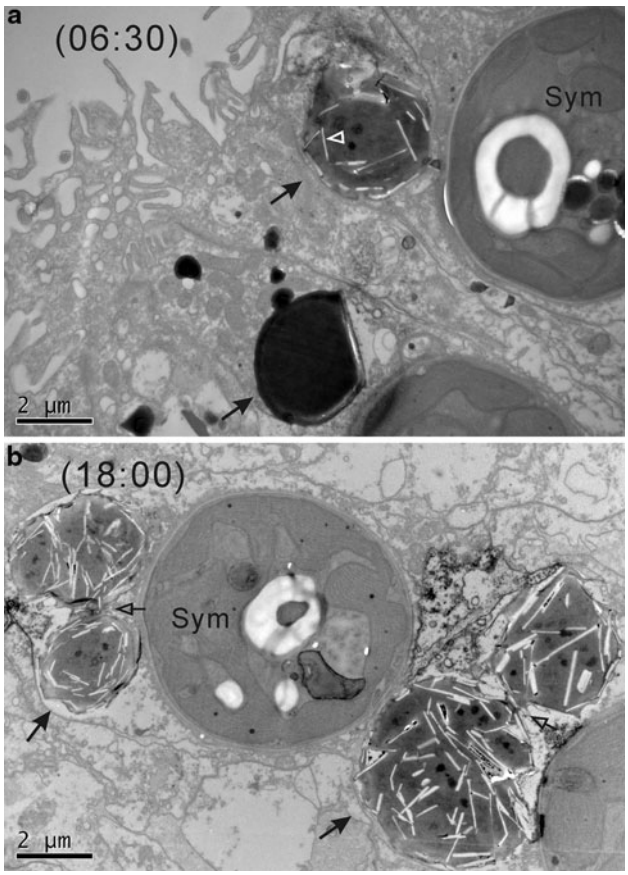

Fig. 5 LB ultrastructural morphology in coral tentacles collected at different times. **a** Gastrodermal LBs at sunrise (06:30 hours) are single globules (see *filled arrows*) with few rectangular electron-transparent inclusion bodies (ETIs) inside the matrix (*blank arrowhead*). **b** At sunset (18:00 hours), both size of LBs (see *filled arrows*) and the ETI number and area increased. Furthermore, connection bridges between LBs (indicated by *blank arrows*) were common. Sym, *Symbiodinium*. A more detailed ultrastructural analysis of LBs from this same coral species can be found in Peng et al. (2011)

Brasaemle 2003). Nevertheless, there are a growing number of concerns with using these fluorescent probes as indicators for lipid droplets (Ohsaki et al. 2010). For instance, the BODIPY 493/503 probe fluoresces green under blue-light excitation. However, when it was used to label lipid droplets in a hepatoma cell line (Huh7), the blue-light excitation during the fluorescence microscopic examination induced a D_{II} dimer formation that resulted in a red fluorescence shift of the BODIPY 493/503 probe (Ohsaki et al. 2010). A similar fluorescence shift was observed when the nile red probe was used to label LBs in the coral gastroderm (personal observation). In addition, autofluorescence from *Symbiodinium* chlorophyll can also interfere with fluorescence microscopy examinations. As a consequence, the use of fluorescent probes for LBs demands particular exposure control in microscopy and is not suitable when an extended period of time is required for observation and image recording, as was necessary in the present study.

Table 1 Temporal changes in LB size and electron-transparent inclusion body (ETI) area from TEM examination

Time	*N*	LB area (μm^2)	Inclusion bodies area (% of LB area)
06:30 (sunrise)	67	3.10 ± 2.34^{a}	1.87 ± 1.18^{a}
09:00	71	3.06 ± 4.33^{a}	12.91 ± 3.02^{b}
12:00	56	$5.37 \pm 4.28^{a,b}$	18.00 ± 2.57^{c}
15:00	51	7.94 ± 5.78b	30.88 ± 2.73^{d}
18:00 (sunset)	118	10.61 ± 7.58c	26.54 ± 1.77^{d}
01:00	47	$4.02 \pm 3.17^{a,b}$	5.22 ± 1.46^{e}
P value		$P < 0.001$	$P < 0.001$

Upper level a to e denotes statistical significance between different times (i.e., 06:30, 09:00, 12:00, 15:00, 18:00, and 01:00) as analyzed by ANOVA. *N* is the number of LBs analyzed

The unique nature of LB formation in coral-*Symbiodinium* endosymbiosis

The results of the present study are summarized schematically in Fig. 7, which highlights the unique nature of LB formation in endosymbiotic coral cells in comparison with cell types from other organisms (Ohsaki et al. 2009). First, coral LB formation appears to result from an interaction between the host gastrodermal cell and *Symbiodinium* (S). Proteomic and ultrastructural analyses have indicated that both *Symbiodinium* and host organelles, such as the ER and mitochondria, are involved in LB biogenesis (Peng et al. 2011). As a consequence, the diel change in LB formation is likely closely related to solar irradiation and concomitant changes in *Symbiodinium* photosynthesis. Specifically, the onset of solar irradiation at sunrise appears to initiate LB formation (step 1, Fig. 7), which is followed by further increases in LB quantity over the course of the day until sunset (steps 2–3). LB density then gradually decreases at night ("nocturnal utilization", step 4), during which time the LBs are potentially metabolized. To further implicate the importance of the light cycle, the temporal dynamics of LB density were concurrent with changes in LB morphology and lipid content. This suggests that there is a circadian maturation process ($\sim$24 h) that may be driven by light-regulated lipid metabolism. Thirdly, the light–dark photoperiod may also influence the spatial distribution of LBs, given the observed LB migration across the gastroderm (steps 1–4). Collectively, these data suggest that solar irradiation may influence the maturation and metabolism of LBs. LB formation occurred in an irradiation-dependent manner, not only during the diel cycle (Fig. 2), but also across different seasons (Fig. 3a). As shown in Fig. 7, the increase in LB density (steps 1–3) is correlated with the diel change in light

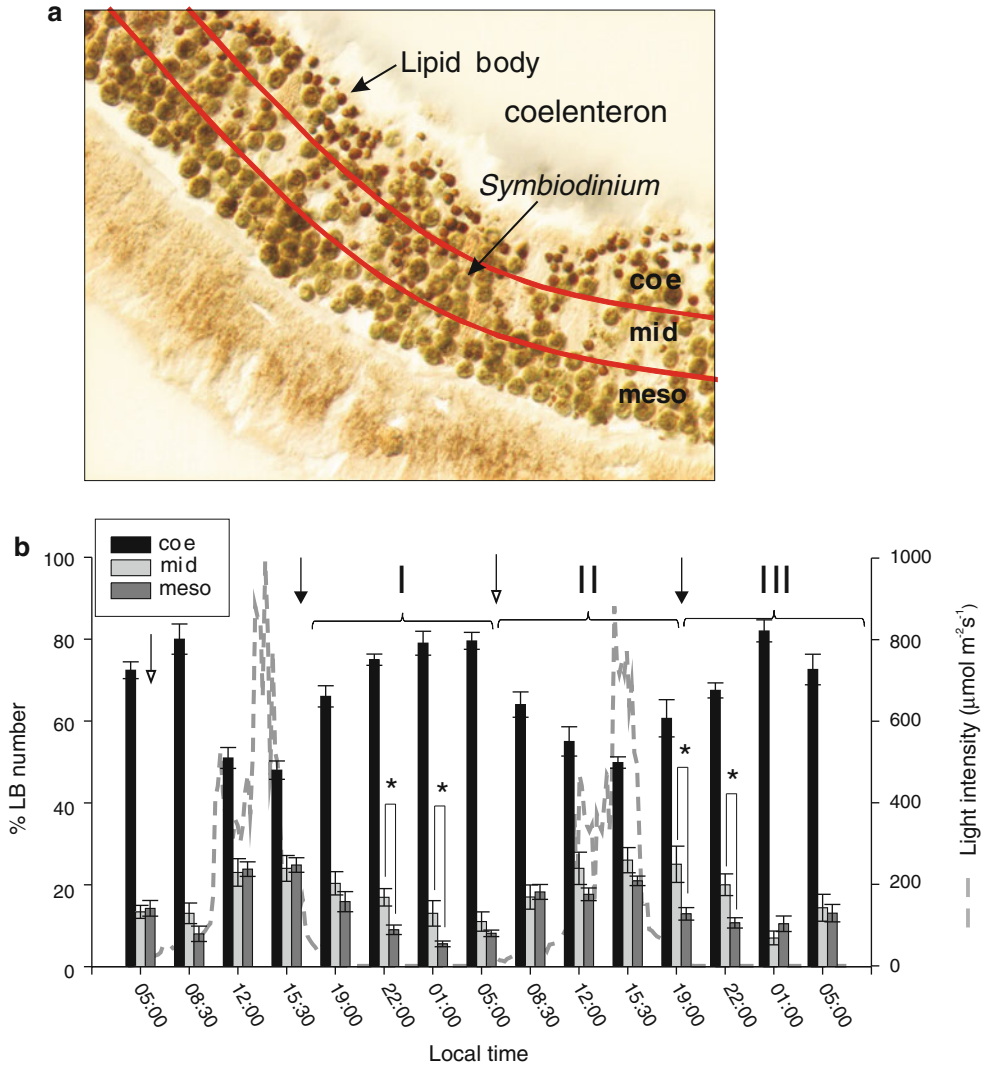

Fig. 6 LB distribution. **a** LB redistribution was demonstrated by calculating the percentage of LBs in each of the three gastrodermal regions; "meso" (the region closest to the mesoglea), "mid" (the middle region of the gastroderm), and "coe" (the region closest to the coelenteron). **b** The average circadian change of the percent (%) LB fraction in each of these three regions was averaged from four individual experiments (April 10th–12th, June 30th–July 1st, and October 8th–9th in 2010, and February 6th–8th in 2011). Ten images from three coral colonies were analyzed at each time point, and no colony was amputated more than once. The light intensity over time is also plotted (*dashed line*). Phases I and III: dark photoperiods (between sunset and sunrise). Phase II: the daytime photoperiod (sunrise to sunset). Data are presented as mean ± SEM ($n = 10$). *Asterisks* ("*") denote statistical significance at $P < 0.05$

intensity, which strongly implicates solar irradiation as a driving force of the lipid flow between the host gastrodermal cell and *Symbiodinium*. LBs, then, may represent one means of transporting lipids within the holobiont.

Temporal regulation of LB biogenesis

At the moment, it is not possible to assess LB utilization by the coral during the daytime due to the simultaneous occurrence of light-driven LB formation (Fig. 2). However, measurements based on LB density change (Fig. 3b) from sunset to sunrise (i.e., the nocturnal period), indicated that ~48–63% of LBs were utilized, and presumably metabolized. Whether seasonal integrated solar irradiation could affect this utilization remain to be elucidated. However, the rate of nocturnal LB disappearance was fastest in spring, when daily integrated light intensity was the highest (Fig. 3c).

The present study not only examined diel changes in gastrodermal LB quantity, but also temporal variation in their lipid composition, specifically with regard to ST, WE, and TG. Although these lipid species have been detected in "extra-algal" lipid droplets in the coral *Stylophora pistillata* (Patton and Burris 1983) and the sea anemone *Condylactis gigantea* (Kellogg and Patton 1983), their weight percentages were markedly different from those of

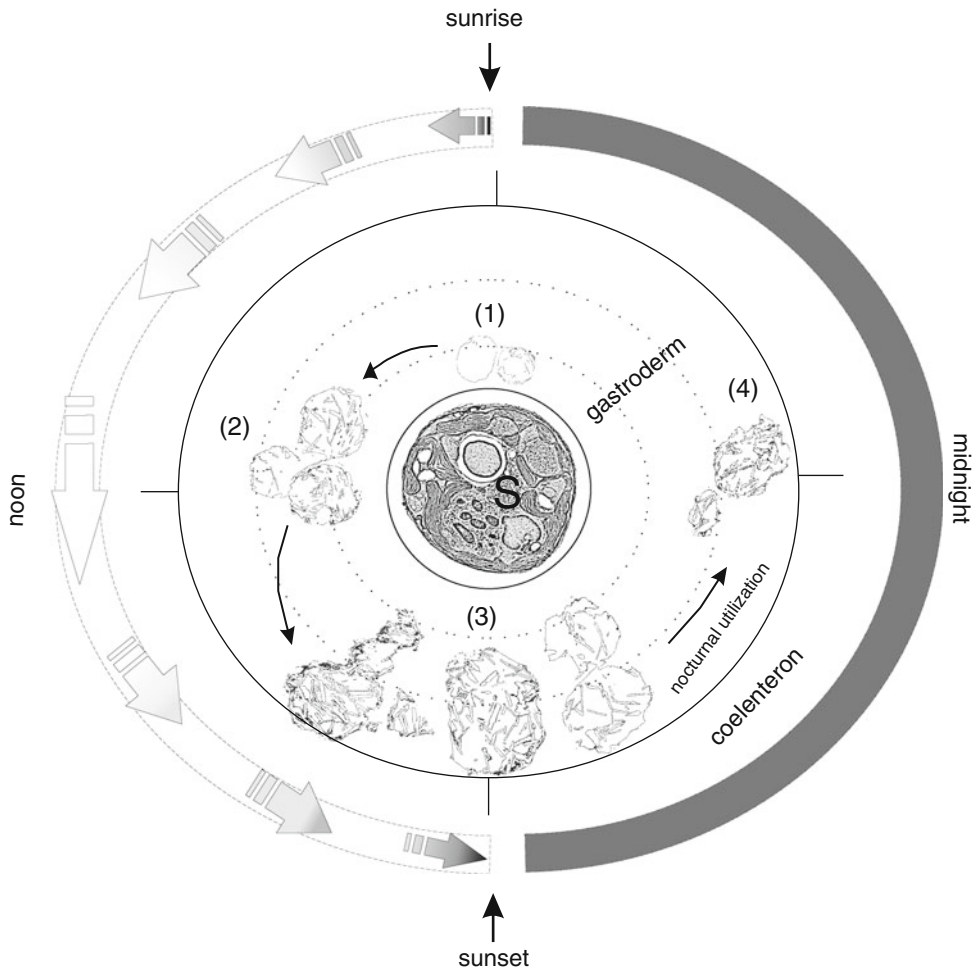

Fig. 7 Schematic summary of the temporal and spatial regulation of LB formation during the diel photoperiod

the present study. In *E. glabrescens* LBs, ST was the dominant lipid species (60–90%), with TG (~20%) and WE (2–10%) contributing smaller proportions to the total lipid pool (Fig. 4d). On the other hand, WE was the major lipid species in the extra-algal lipid droplets of *Condylactis gigantea* (83.4%; Kellogg and Patton 1983), and TG was the major species in extra-algal lipid droplets of *Stylophora pistillata* (~75%; Patton and Burris 1983). However, it is likely that these lipid droplets were actually host nuclei (Muscatine et al. 1994).

Similarly, previous studies showed that the rates of ^{14}C-incorporation into TG and WE were significantly different, suggesting different metabolic pathways (Crossland et al. 1980). In *E. glabrescens* LBs, only the concentration (weight%) of WE exhibited a diel change (inset of Fig. 4d), while TG and ST levels remained similar over time. This observation may provide insight into understanding LB lipid metabolism. In particular, it suggests that LB lipids come from different sources and that their metabolism and accumulation are differentially regulated.

The diel change of LB density was also concurrent with morphological changes in individual LB, a characteristic not being observed in lipid droplets of other eukaryotic cells (Tauchi-Sato et al. 2002; Ohsaki et al. 2009). Two striking morphological characteristics of coral gastrodermal LBs are their diel variations in size and ETI bodies (Fig. 5; Table 1). Regarding to the former, while the regulation of coral LB size remains to be elucidated, the current results suggest that the size increase during the day is resulted from the LB fusion (Fig. 5b). In fact, LBs with irregular shapes resulting from this fusion were frequently observed in tentacles sampled at sunset, as illustrated by Fig. 7 (step 3).

Although the composition of ETIs in LBs was not determined in the present study, WE has been shown to be their major component in other cells, including bacteria and cnidarians (Vandermeulen 1974; Crossland et al. 1980; Ishie et al. 2002). It is also important to note that the diel change in WE concentration (Fig. 4d) correlated with the ETI area (Table 1), and both peaked at sunset (Fig. 7, steps 1–3). It is possible, then, that accumulation and synthesis of TG and WE are differentially regulated. The accumulation of WE within ETIs at sunset seems to signal the completion of LB maturation.

Spatial regulation of LB biogenesis

Imaging analyses (Fig. 6) showed that LB populations migrate across the gastroderm during the diel cycle (Fig. 7, steps 1–4). The mechanism for this redistribution remains unknown. Although amputated tentacles had been relaxed by anaesthetizing with 7% $MgCl_2$, the sectioned gastroderm still showed multiple layers of cells containing endosymbionts (see Figs. 1c–f, 6a). It is quite feasible, then, that there is a time-dependent relocation of LBs inside a single gastrodermal cell during their biogenesis that ultimately manifests as an apparent redistribution of LBs across the gastrodermal tissue layer.

Lipid droplets have been shown to migrate along cytoskeletal elements during the growth and disintegration (Welte 2007). Proteomic analyses further indicated the important role of the cytoskeleton in coral LBs, as 21% of the LB-associated proteins of *E. glabrescens* were cytoskeleton-related proteins, including actins, tubulins, and their binding proteins (Peng et al. 2011). The elucidation of the purpose of LB migration and their interaction with the cytoskeleton and other cellular organelles such as mitochondria and ER during the diel cycle remains a challenge for future study. Interestingly, a previous study of the sea anemone *Condylactis gigantea* found "lipid droplets" to be secreted into the tentacle coelenteron (Kellogg and Patton 1983). Nevertheless, preliminary results showed that only ~1–1.7% of the gastrodermal LBs in *E. glabrescens* were secreted during the night (personal observation), so, while they are highly mobile within the coral tissue, a far greater proportion are utilized by the coral than released into the seawater (Fig. 3b).

The present data demonstrate the dynamics of LB formation in coral gastrodermal tissues, uncovering lipid compositional and ultrastructural changes characterized with a diel rhythmicity. Further examinations on the cellular sources of LB lipids and how they are regulated during the diel cycle will provide important insight toward understanding the molecular mechanisms underlying stable cnidarian–dinoflagellate endosymbioses.

Acknowledgments This work was supported by a grant from the National Science Council of Taiwan (NSC 98-2311-B-291-001-MY3) and by intramural funding from NMMBA (99200311). ABM was supported by an international postdoctoral research fellowship (OSE-0852960) from the National Science Foundation of the United States of America.

References

Abe A (1998) Modification of the Coomassie brilliant blue staining method for sphingolipid synthesis inhibitors on silica gel thin-layer plate. Anal Biochem 258:149–150

Bligh EG, Dyer WJ (1959) A rapid method of total lipid extraction and purification. Can J Biochem Physiol 37:911–917

Cermelli S, Guo Y, Gross SP, Welte MA (2006) The lipid-droplet proteome reveals that droplets are a protein-storage depot. Curr Biol 16:1783–1795

Cheng J, Fujita A, Ohsaki Y, Suzuki M, Shinohara Y, Fujimoto T (2009) Quantitative electron microscopy shows uniform incorporation of triglycerides into existing lipid droplets. Histochem Cell Biol 132:281–291

Crossland CJ, Barnes DJ, Borowitzka MA (1980) Diurnal lipid and mucus production in the staghorn coral *Acropora acuminata*. Mar Biol 60:81–90

D'Avila H, Melo RCN, Parreira GG, Werneck-Barroso E, Castro-Favia-Neto HC, Bozza PT (2006) *Mycobacteriium bovis* Bacillus Calmette-Guerin induces TLR2-mediated formation of lipid bodies: intracellular domains for eicosanoid synthesis in vivo. J Immunol 176:3087–3097

DiDonato D, Brasaemle DL (2003) Fixation methods for the study of lipid droplets by immunofluorescence microscopy. J Histochem Cytochem 51:773–780

Duncan RE, Ahmadian M, Jaworski K, Sarkadi-Nagy E, Sul HS (2007) Regulation of lipolysis in adipocytes. Annu Rev Nutr 27:79–101

Fowler SD, Greenspan P (1985) Application of nile red, a fluorescent hydrophobic probe, for the detection of neutral lipid deposits in tissue sections: comparison with oil red o. J Histochem Cytochem 33:833–836

Fuchs B, Schiller J, Sub R, Schurenberg M, Suckau D (2007) A direct and simple method of coupling matrix-assisted laser desorption and ionization time-of-flight mass spectrometry (MALDI-TOF MS) to thin-layer chromatography (TLC) for the analysis of phospholipids from egg yolk. Anal Bioanal Chem 389:827–834

Fujimoto Y, Itabe H, Sakai J, Makita M, Noda J, Mori M, Higashi Y, Kojima S, Takano T (2004) Identification of major proteins in the lipid droplet-enriched fraction isolated from the human hepatocyte cell line HuH7. Biochim Biophys Acta 1644:47–59

Ishie T, Tani A, Takabe K, Kawasaki K, Sakai Y, Kato N (2002) Wax ester production from n-alkanes by *Acinetobacter* sp. strain M-1: ultrastructure of cellular inclusions and role of acyl coenzyme A reductase. Appl Environ Microbiol 68:1192–1195

Kellogg RB, Patton JS (1983) Lipid droplets: medium of energy exchange in the symbiotic anemone *Condylactis gigantea*, a model coral polyp. Mar Biol 75:137–149

LaJeunesse TC, Smith R, Walther M, Pinzón J, Pettay DT, McGinley M, Aschaffenburg M, Medina-Rosas P, Cupul-Magaña AL, Pérez AL, Reyes-Bonilla H, Warner ME (2010) Host-symbiont recombination versus natural selection in the response of coral-dinoflagellate symbioses to environmental disturbance. Proc R Soc B 277:2925–2934

Liu P, Ying Y, Zhao Y, Mundy DI, Zhu M, Anderson RGW (2004) Chinese hamster ovary K2 cell lipid droplets appear to be metabolic organelles involved in membrane traffic. J Biol Chem 279:3787–3792

Luo YJ, Wang LH, Chen WNU, Peng SE, Tzen JTC, Hsiao YY, Huang HJ, Fang LS, Chen CS (2009) Ratiometric imaging of gastrodermal lipid bodies in coral-dinoflagellate endosymbiosis. Coral Reefs 28:289–301

Mastro R, Hall M (1999) Protein delipidation and precipitation by tri-n-butylphosphate, acetone, and methanol treatment for isoelectric focusing and two dimensional gel electrophoresis. Anal Biochem 273:313–315

Maxfield FR, Tabas I (2005) Role of cholesterol and lipid organization in disease. Nature 438:612–621

Muscatine L, Gates RD, LaFontaine I (1994) Do symbiotic dinoflagellates secrete lipid droplets? Limnol Oceanogr 39:925–929

Ohsaki Y, Cheng J, Suzuki M, Shinohara Y, Fujita A, Fujimoto T (2009) Biogenesis of cytoplasmic lipid droplets: from the lipid ester globule in the membrane to the visible structure. Biochim Biophys Acta 1791:399–407

Ohsaki Y, Shinohara Y, Suzuki M, Fujimoto T (2010) A pitfall in using BODIPY dyes to label lipid droplets for fluorescence microscopy. Histochem Cell Biol 133:477–480

Oku H, Yamashiro H, Onaga K (2003) Lipid biosynthesis from [^{14}C]-glucose in the coral *Montipora digitata*. Fish Sci 69:625–631

Olofsson SO, Bostrom P, Andersson L, Rutberg M, Perman J, Boren J (2009) Lipid droplets as dynamic organelles connecting storage and efflux of lipids. Biochim Biophys Acta 1791:448–458

Ozeki S, Cheng J, Tauchi-Sato K, Hatano N, Taniguchi H, Fujimoto T (2005) Rab18 localizes to lipid droplets and induces their close apposition to the endoplasmic reticulum-derived membrane. J Cell Sci 118:2601–2611

Patton JS, Burris JE (1983) Lipid synthesis and exclusion by freshly isolated zooxanthellae (symbiotic algae). Mar Biol 75:131–136

Patton JS, Battey JF, Rigler MW, Porter JW, Black CC, Burris JE (1983) A comparison of the metabolism of bicarbonate 14C and acetate 1–14C and the variability of species lipid compositions in reef corals. Mar Biol 75:121–130

Peng SE, Luo YJ, Huang HJ, Lee IT, Hou LS, Chen WNU, Fang LS, Chen CS (2008) Isolation of tissue layers in hermatypic corals by N-acetylcysteine: morphological and proteomic examinations. Coral Reefs 27:133–142

Peng SE, Wang YB, Wang LH, Chen WNU, Lu CY, Fang LS, Chen CS (2010) Proteomic analysis of symbiosome membranes in cnidaria-dinoflagellate endosymbiosis. Proteomics 10:1002–1016

Peng SE, Chen WNU, Chen HK, Lu CY, Mayfield AB, Fang LS, Chen CS (2011) Lipid bodies in coral-dinoflagellate endosymbiosis: proteomic and ultrastructural studies. Proteomics 17:3540–3555

Prattes S, Hörl G, Hammer A, Blaschitz A, Graier WF, Sattler W, Zechner R, Steyrer E (2000) Intracellular distribution and mobilization of unesterified cholesterol in adipocytes: triglyceride droplets are surrounded by cholesterol-rich ER-like surface layer structures. J Cell Sci 113:2977–2987

Robenek H, Hofnagel O, Buers I, Robenek MJ, Troyer D, Severs NJ (2006) Adipophilin-enriched domains in the ER membrane are sites of lipid droplet biogenesis. J Cell Sci 119:4215–4224

Tauchi-Sato K, Ozeki KS, Honjou T, Taguchi R, Fujimoto T (2002) The surface of lipid droplets is a phospholipid monolayer with a unique fatty acid composition. J Biol Chem 277:44507–44512

Umlauf E, Császár E, Moertelmaier M, Schuetz GJ, Parton RG, Prohaska R (2004) Association of stomatin with lipid bodies. J Biol Chem 279:23699–23709

Vandermeulen JH (1974) Studies on reef corals, II. Fine structure of planktonic planula larva of *Pocillopora damicornis*, with emphasis on the aboral epidermis. Mar Biol 27:239–249

Wan HC, Melo RCN, Jin Z, Dvorak AM, Weller PF (2007) Roles and origins of leukocyte lipid bodies: proteomic and ultrastructural studies. FASEB J 21:167–178

Weis VM, Allemand D (2009) What determines coral health? Science 324:1153–1155

Weis VM, Davy SK, Hoegh-Guldberg O, Rodriguez-Lanetty M, Pringle JR (2008) Cell biology in model systems as the key to understanding corals. Trends Ecol Evol 23:369–376

Welte MA (2007) Proteins under new management: lipid droplets delivery. Trends Cell Biol 17:363–369

Whitehead LF, Douglas AE (2003) Metabolite comparisons and the identity of nutrients translocated from symbiotic algae to an animal host. J Exp Biol 206:3149–3157